

Determination of the Carrier-Envelope Phase of Few-Cycle Laser Pulses with Terahertz-Emission Spectroscopy

Markus Kriebel¹, Torsten Löffler¹, Mark D. Thomson¹, Reinhard Dörner², Hartmut Gimpel³, Karl Zrost³, Thorsten Ergler³, Robert Moshhammer³, Uwe Morgner^{3,4}, Joachim Ullrich³, and Hartmut G. Roskos¹

¹ *Physikalisches Institut, Johann Wolfgang Goethe-Universität,
Max-von-Laue-Str. 1, D-60438 Frankfurt (M), Germany*

² *Institut für Kernphysik, Johann Wolfgang Goethe-Universität,
Max-von-Laue-Str. 1, D-60438 Frankfurt (M), Germany*

³ *Max-Planck-Institut für Kernphysik, Saupfercheckweg 1, D-69117 Heidelberg, Germany*

⁴ *Institut für Quantenoptik, D-30167 Hannover, Germany and
Correspondence should be addressed to - [MK]*

(Dated: March 16, 2006)

PACS numbers: 42.65.-k, 62.65.Re, 72.30.+q

The availability of few-cycle optical pulses opens a window to physical phenomena occurring on the attosecond time scale. In order to take full advantage of such pulses, it is crucial to measure^{1,2,3,4} and stabilise^{1,2} their carrier-envelope (CE) phase, i.e., the phase difference between the carrier wave and the envelope function. We introduce a novel approach to determine the CE phase by down-conversion of the laser light to the terahertz (THz) frequency range via plasma generation in ambient air, an isotropic medium where optical rectification (down-conversion) in the forward direction is only possible if the inversion symmetry is broken by electrical or optical means^{5,6,7,8,9,10}. We show that few-cycle pulses directly produce a spatial charge asymmetry in the plasma. The asymmetry, associated with THz emission, depends on the CE phase, which allows for a determination of the phase by measurement of the amplitude and polarity of the THz pulse.

The ability to measure^{1,2,3,4} and stabilise^{1,2} the CE phase, which is also often named absolute phase and defined by Eq. 4 (Methods), of few-cycle laser pulses, i.e., the ability to completely control ultrashort high-intensity electromagnetic fields, provides access to a whole series of novel physical phenomena, and creates options for their coherent control. An example is the manipulation of the electron recombination process during “re-collision”¹¹, with the aim to fully control the generation of both intense VUV higher-harmonic radiation^{12,13} as well as of high-intensity single attosecond pulses. The progress has led to the establishment of a new field of research, “attosecond science”, with highlights of recent work including the efficient tomography of molecular wave functions by coherent diffraction of rescattered electrons¹⁴ as well as the preparation of high-intensity, monochromatic femtosecond electron beams evolving from “bubble generation”¹⁵. Many of the phenomena studied depend critically on the CE phase. Examples include the dynamics of above-threshold ionisation (ATI)⁴, light-induced non-sequential double ionisation¹⁶, Gouy phase observation¹⁷, and quantum interference in

photocurrents¹⁸. An exciting prospect is the application of the CE phase as a coherent-control tool, e.g., to steer bound electrons in molecules¹⁹.

The state-of-the-art method for CE phase determination of amplified laser pulses is stereo ATI^{20,21}. In this letter, we present a new approach based on down-conversion into the THz frequency range in a laser-generated ambient air-plasma. The concept relies on the detection of the THz electromagnetic pulses emitted during photo-ionization of the air by the focussed few-cycle pulses. The method is easy to apply, because it does not require a vacuum chamber and relies on standard optoelectronic THz detection technology^{5,8}.

THz-pulse emission from laser-generated plasmas has been investigated in the past, but only with much longer laser pulses. There, the transient electric currents responsible for the THz radiation have their origin either in ponderomotive forces²², the Coulomb force of an externally applied DC bias^{5,6}, or an optical “AC bias” achieved by superimposing the light pulses with their own second-harmonic radiation^{7,8,9,10}. The THz-wave generation mechanism for the latter has been discussed in terms of a four-wave-mixing (FWM) process^{7,9,10}. For the present case where the pulse spectra are octave-spanning FWM results in a low-frequency ($\Omega \rightarrow 0$) polarisation: $P(\Omega = \omega_1 + \omega_2 - \omega_3) \propto \sqrt{I(\omega_1)I(\omega_2)I(\omega_3)} \cos(\varphi_{CE})$, because the CE phases φ_{CE} of all three input waves are the same (as all frequency components arise from the same near-transform-limited few-cycle pulse). The CE phase is hence directly imparted onto the single-cycle THz pulse and can thus be determined via electrooptic measurement of the THz field amplitude. The same argument concerning the transfer of the CE phase to the THz field can be readily generalised to the case of higher-order non-linear contributions.

Whilst such a wave-mixing process illustrates the mechanism for CE phase-sensitive THz generation, we will give an alternative description based on static-tunnelling theory²³, which explains the origin of non-linear polarisation on a microscopic level. For simplicity, we assume the air to consist only of N₂. Figure 1 displays the calculated

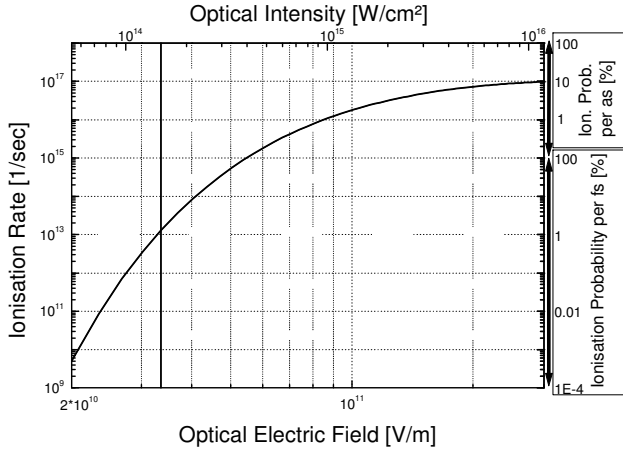


FIG. 1: Ionisation rate for N_2 vs. electric field strength based on the static-tunnelling theory as a function of the optical field strength, respectively the light intensity. The calculation was performed with the help of Eq. 1 of Sec. I. An ionisation rate of 10^{15} s^{-1} corresponds to a probability of 100 % for a molecule to be ionised during a time interval of 1 fs. Note, that the probability for ionisation of a molecule has a value of 1% per fs at a threshold field of $3.3 \cdot 10^{10} \text{ V/m}$ (vertical black line), and that the ionisation probability per fs already becomes 100% at $5.5 \cdot 10^{10} \text{ V/m}$, i.e., at less than twice the threshold field.

ionisation rate w_{tun} for N_2 at a pressure of 1 atm, respectively the ionisation probability rate of a single molecule. The strongly non-linear intensity dependence of the ionisation rate translates into temporal ionisation patterns as illustrated in Fig. 2. The upper panels display the two pulse shapes considered here, both with the same pulse duration of $\tau = 6 \text{ fs}$ (FWHM), the same centre wavelength of $\lambda = 800 \text{ nm}$, and the same peak electric field of the envelope of $E_{opt}^0 = 4.2 \cdot 10^{10} \text{ V/m}$, but with different CE phases, $\varphi_{CE} = 0$ and $\varphi_{CE} = \pi/2$. The middle panels of Fig. 2 exhibit the time evolution of the ionisation rates for the two cases. A common signature is that only the three or four most intense half-cycles of the pulses ionise a significant amount of molecules. The ionisation rate at each half-cycle, however, depends sensitively on the CE phase. This becomes even clearer when we calculate the temporal evolution of the plasma density. We distinguish two quantities, $\rho^+(t)$ and $\rho^-(t)$, which describe the densities of free electrons produced at positive and negative polarity of the optical laser field, respectively. The total density of free electrons is given by $\rho_{total} = \rho^+(t) + \rho^-(t)$. The lower pair of panels of Fig. 2 shows that for $\varphi_{CE} = 0$, the total plasma density generated at negative field polarity is significantly smaller than the density for positive polarity. For $\varphi_{CE} = \pi/2$, the densities only differ little after the pulse has passed through the focus.

Electrons generated at positive field polarity experience a displacement in the positive field direction due to acceleration in the laser field and incoherent scattering at neighbouring molecules within a few fs. Cor-

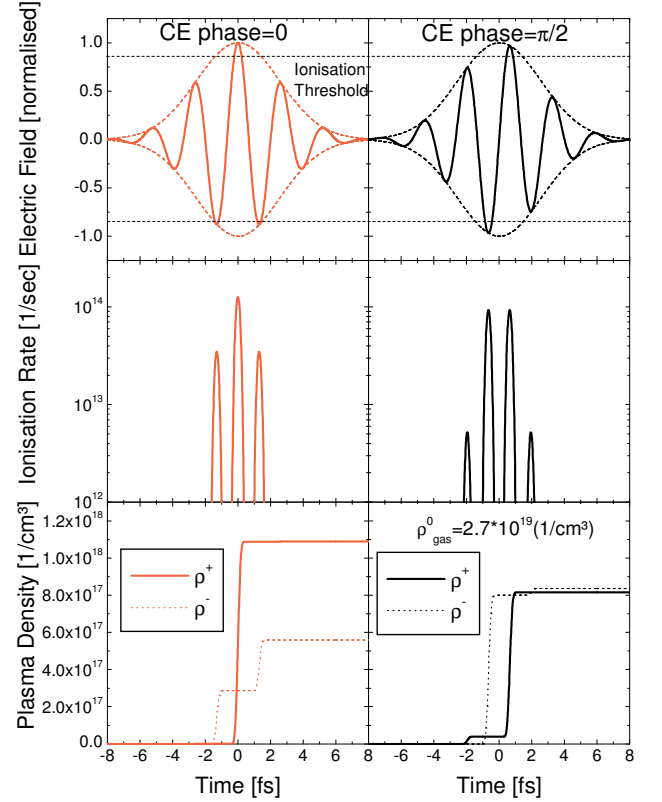


FIG. 2: Optical electric field, ionisation rate and plasma densities as a function of time for CE phases $\varphi_{CE} = 0$ and $\varphi_{CE} = \pi/2$. The plasma densities ρ^+ and ρ^- , generated at positive respectively negative field polarities, are calculated with Eqs. 2 and 3 of Sec. I. The ionisation threshold is the arbitrarily chosen electric-field value where the ionisation probability is 1% per fs.

respondingly, electrons generated at negative polarity are displaced in the negative direction. Such a collective charge displacement after the passage of the pulse ($\lim_{t \rightarrow \infty} (\rho^+(t) - \rho^-(t)) \neq 0$), creates a quasi-DC macroscopic dipole moment. Because of its transient character, it acts as the source of an electromagnetic pulse, whose polarity and field amplitude are determined by the ratio $R_\rho^\infty = \lim_{t \rightarrow \infty} ((\rho^+ - \rho^-)/(\rho^+ + \rho^-))$, a quantity which is proportional to the maximal generated dipole moment. A value of $R_\rho^\infty = \pm 1$ corresponds to the highest possible THz pulse amplitude, with the polarity of the signal depending on the sign of R_ρ^∞ . For $R_\rho^\infty = 0$, THz emission vanishes. Figure 3 displays R_ρ^∞ as a function of φ_{CE} for laser pulses with Gaussian envelope of various durations τ . One finds that the magnitude of R_ρ^∞ is directly related to the CE phase with a nearly cosine-like dependence. The contrast, however, rapidly vanishes when the pulse duration rises towards 10 fs.

Whilst the theory for stereo ATI requires modelling of both the quiver motion and recollision of electrons, this is not necessary for THz emission from a plasma generated at atmospheric pressure. The reason for this is

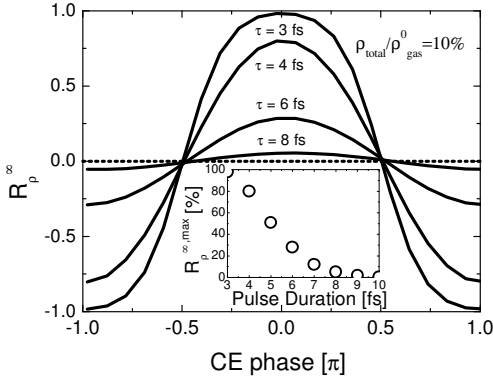


FIG. 3: Asymmetry parameter R_ρ^∞ of the plasma density vs. CE phase for several pulse durations. R_ρ^∞ is proportional to the macroscopic quasi-DC dipole moment which is responsible for the emission of the THz radiation. The pulse intensity is chosen such that a plasma density ρ_{total} of 10% of the molecule density ρ_{gas}^0 is obtained. Inset: Maximal value of R_ρ^∞ at $\varphi_{CE} = 0$ as a function of the pulse duration.

that the coherent motion of the majority of electrons is terminated by ultrafast scattering before recollision and the THz signal is proportional to the asymmetry in the tunnelling process. Therefore the signal in our method is conceptually and in contrast to stereo ATI directly related to the CE phase in a way such that a cosine-like pulse ($\varphi_{CE} = 0$) will produce a maximum asymmetry in ionisation rates and also a maximum THz-signal. The introduced THz method would measure directly the absolute CE phase, if the plasma would be a point object. However, the plasma is an extended object²⁴ and we expect a CE phase variation by dispersion during pulse propagation and a concomitant interference of the THz signals generated along the beam path. The strength of this effect for the moment is unknown, but will be investigated in future measurements and simulations.

An experimental test of these theoretical findings was performed by THz-emission spectroscopy with phase-stabilised 8-fs amplified laser pulses (see in Methods a detailed description of the set-up displayed in Fig. 4). We measured the THz field value from a laser-generated air plasma at a fixed temporal position (that with the largest amplitude of the THz transients) while continuously varying the CE phase by slowly ramping the set-point of the control loop (with a slope of 2π per minute). An exemplary time series spanning 8 minutes is shown in Fig. 5a. The CE phase data measured in the frequency domain by two f-to-2f interferometers² (CEP2 and CEP3) are compared to the THz data. The THz signal varies with the ramped CE phase, as expected from the model calculations shown in Fig. 3.

In a second experiment, the CE phase was kept constant in the oscillator and laser amplifier (CEP2), but varied with the help of a piezo-driven glass-wedge pair behind the pulse compressor and in front of both the

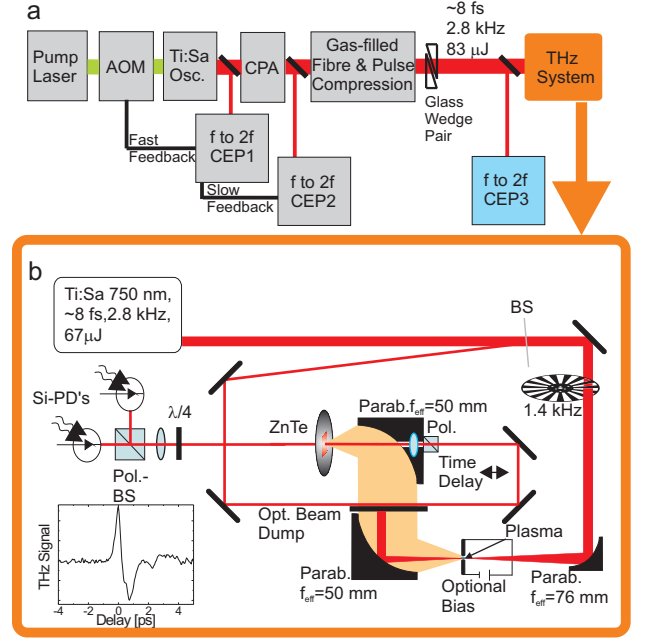


FIG. 4: Sketch of the Experimental set-up. a) Schematic of the laser system. AOM, acousto-optical modulator; CEP1, f-to-2f interferometer used for CE phase stabilisation with fast feedback; CPA, chirped pulse amplification and compression; CEP2, f-to-2f interferometer used for compensation of slow drifts of the CE phase; gas-filled fibre used for spectral broadening; CEP3, f-to-2f interferometer only used for CE phase measurements; b) THz system employed for electro-optical THz detection. Inset: A temporal THz wave-form obtained with applied DC bias.

third f-to-2f interferometer (CEP3) and the THz system (also with a phase ramping of 2π per minute). The results are depicted in Fig. 5b. The measurements again consolidate the expected change of the THz signal with varying CE phase.

In order to provide a more quantitative analysis of the measurements, we show in Fig. 5c the THz signal as a function of the CEP3 data (open dots), averaged over a 74-minute time series, where we ramped the phase of the oscillator as in Fig. 5a. The error bar indicates the standard deviation of the THz-signal values. The correlation between THz signal and CEP3 compares well with the dependence predicted in Fig. 3 for 8-fs pulses (full line in Fig. 5c). The slight deviation of the theoretical data from the experimental ones may be a consequence of a non-Gaussian shape of the envelope.

The status of the THz approach for CE phase determination can be considered as a proof-of-principle. Nevertheless, to classify its current precision, we compare it to stereo ATI, which achieves a 3σ error of 100 mrad for 10 seconds of data acquisition and for 6.5-fs 20- μ J pulses²¹. The precision reached with the THz system is 700 mrad

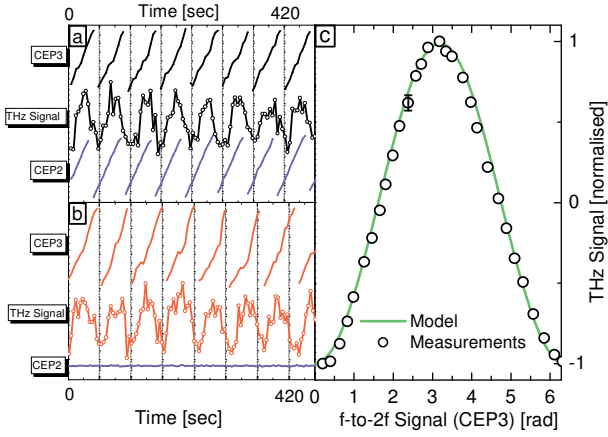


FIG. 5: a) Variation of the CE phase of 8-fs pulses obtained by slowly ramping the set-point of the control loop. The CE phase is measured by a f-to-2f interferometer (CEP2) directly behind the laser amplifier, another f-to-2f interferometer (CEP3) behind the recompressor, and by the THz measurement system via electro-optical detection of the THz radiation generated in an ambient air plasma. The integration time constant of the lock-in amplifier in the THz measurements was 100 ms. In addition, a sliding average was calculated numerically, bringing the effective integration time constant to 5 sec. Dispersion effects result in an arbitrary offset between the CE phases measured by CEP2, CEP3 and the THz system. b) Variation of the CE phase of 8-fs pulses by a change of the dispersion in the beam path, realised by two variable glass wedges. c) Adjacent average of the correlation of the CEP3 and the THz data. The window chosen for averaging was ± 0.5 radians of CEP3. For the averaging, the total data pool recorded within 74 min. is taken into account. The error bar depicts the standard deviation of this averaging. The solid line shows the results of model calculations of R_{ρ}^{∞} for an 8-fs pulse (constant scaling factor between theory and experiment). The peak electric field used for calculations is $E_{opt}^0 = 4 \cdot 10^{10}$ V/m corresponding to the expected value in the experiment.

for 10 seconds of data acquisition for 8-fs 66- μ J pulses. Considering the factor-of-4 improvement to be achieved with 6.5-fs instead of 8-fs pulses (see Fig. 3), the THz approach compares well with the much more mature ATI method already now. The sensitivity of low-repetition-rate THz-detection can be enhanced significantly by boxcar techniques or by THz interferometry with intensity detection over a large THz-photon bandwidth.

In summary, we report (i) frequency down-conversion in an isotropic medium without breaking the symmetry of the non-linear medium by external means, and (ii) CE phase measurement of sub-10-fs amplified optical pulses, both by detection of the THz radiation emitted from a laser-generated ambient-air plasma. The theory of tunnelling ionisation explains the findings well, in particular the down-conversion (THz generation) by a spatially asymmetric process of ionisation and charge acceleration. THz-emission spectroscopy possesses the potential to be-

come a commonly employed tool for determination and long term stabilisation of the CE phase for amplified few-cycle pulses.

I. METHODS

Ionisation model employed in the simulations

We base the quantitative description of the photo-ionisation process of atoms and molecules on static-tunnelling theory²³, with the following expression for the ionisation rate:

$$w_{tun} = 4\omega_a \left(\frac{U_{ion}^{N_2}}{U_{ion}^H} \right)^{\frac{5}{2}} \left(\frac{E_a}{E_{opt}} \right) \times \exp \left(-\frac{2}{3} \left(\frac{U_{ion}^{N_2}}{U_{ion}^H} \right)^{\frac{3}{2}} \left(\frac{E_a}{E_{opt}} \right) \right), \quad (1)$$

where $\omega_a = 4.13 \cdot 10^{16}$ 1/s is the atomic frequency unit, $E_a = 5.145 \cdot 10^{11}$ V/m the atomic unit of the electric field, and E_{opt} the optical field strength. $U_{ion}^H = 13.6$ eV and $U_{ion}^{N_2} = 15.6$ eV denote the ionisation potentials of atomic hydrogen and molecular nitrogen, respectively. The simple tunnelling model is known to describe the experimental data for N_2 well if the intensity of the laser pulses is above 10^{14} W/cm², and to achieve a fair agreement down to $5 \cdot 10^{13}$ W/cm²²⁵.

Temporal evolution of the ionisation

In order to determine the temporal evolution of the plasma current, we compute the plasma densities $\rho^+(t)$ and $\rho^-(t)$ by solving the following coupled differential equations:

$$\frac{d}{dt} \rho^+(t) = \begin{cases} w_{tun}(E_{opt}(t)) \cdot (\rho_{gas}^0 - \rho^+(t) - \rho^-(t)), & \text{if } E_{opt}(t) \geq 0 \\ 0, & \text{if } E_{opt}(t) < 0, \end{cases} \quad (2)$$

$$\frac{d}{dt} \rho^-(t) = \begin{cases} w_{tun}(E_{opt}(t)) \cdot (\rho_{gas}^0 - \rho^+(t) - \rho^-(t)), & \text{if } E_{opt}(t) < 0 \\ 0, & \text{if } E_{opt}(t) \geq 0. \end{cases} \quad (3)$$

Here, $\rho_{gas}^0 = 2.7 \cdot 10^{19}$ cm⁻³ is the density of N_2 molecules at atmospheric pressure assuming air to only consist of N_2 . $E_{opt}(t)$ denotes the electric field strength of the laser pulse. We neglect plasma recombination which occurs on a much longer time scale²⁶. We assume the following temporal wave-form of the laser pulse:

$$E_{opt}(t) = E_{opt}^0 A(t) \cos \left(\frac{2\pi c}{\lambda} t + \varphi_{CE} \right), \quad (4)$$

where $A(t)$ is a Gaussian envelope. Whilst such a product separation of carrier and envelope can become ill-defined as the pulse duration approaches the sub-cycle range²⁷,

it is perfectly reasonable for the shortest pulse durations we consider here.

Light source

The experiments were performed with a light source as sketched in Fig. 4a. A commercial available Ti:Sapphire Multipass CPA System “Femtopower Compact Pro” (Femtolasers, Vienna) is seeded with a self-build laser oscillator (pulse energy 4 nJ, pulse duration 20fs, centre wavelength 810 nm, CE phase-stabilised with f-to-2f self referencing¹ (CEP1)) and driven at a repetition rate of 2.8 kHz. Its output (500 μ J, 30fs, @805 nm) is focused into a gas-filled hollow fibre (inner diameter 200 μ m, length 82 cm, 4.5 bar Neon). A small fraction of the CPA output (few μ J) are used for a f-to-2f interferometer² (CEP2) to correct for slow CE phase drifts in the amplifier. The fibre output is then compressed to its bandwidth limited duration of 8 fs by the use of dispersive mirrors and a prism-compressor sequence with two fused silica prisms, with final output parameters (83 μ J, 8 fs, @750 nm (centre wavelength)).

THz-emission spectroscopy system

80% of the final output is fed into the THz detection set-

up, which is sketched in Fig. 4b. 10% (the residual 10% are unused) is used for a third f-to-2f interferometer² (CEP3), which is tracing CE phase changes for direct comparison with the THz data in respect to a constant arbitrary offset. The THz system is a typical THz pump-probe measurement system with balanced electro-optical THz detection^{5,8}, the whole set-up is fitting on a 30 \times 45-cm² breadboard. The pump beam is mechanically chopped at half the laser repetition rate. The plasma is generated in the focus of an off-axis paraboloidal mirror with an effective focal length of 76 mm. For optimisation of the alignment and a first determination of the zero-delay point for the THz detection, an additional DC bias field can be applied to the focal region⁵. The probe beam passes along a variable delay line and is focused collinearly with the THz beam into the electro-optical ZnTe detector crystal. The THz wave-form as measured with a DC-biased air plasma is depicted in the lower left part of Fig. 4b. For the CE phase measurements, the delay stage of the probe beam is positioned at the zero-delay point where the strongest THz signal is obtained, and the external bias field is switched off.

-
- ¹ Baltuška, A. *et al.* Attosecond control of electronic processes by intense light fields. *Nature* **421**, 611-615 (2003).
- ² Baltuška, A. *et al.* Phase-Controlled Amplification of Few-Cycle Laser Pulses, *IEEE J. of selected Topics in Quant. Elec.* **9**, 972-989 (2003).
- ³ Apolonski, A. *et al.* Observation of light-phase-sensitive photoemission from a metal. *Phys. Rev. Lett.* **92**, 073902 (2004).
- ⁴ Paulus, G. G. *et al.* Absolute-phase phenomena in photoionization with few-cycle laser pulses. *Nature* **414**, 182-184 (2001).
- ⁵ Löffler, T., Jacob, F., and Roskos, H. G. Generation of terahertz pulses by photoionization of electrically biased air. *Appl. Phys. Lett.* **77**, 453-455 (2000).
- ⁶ Löffler, T. and Roskos, H. G. Gas-pressure dependence of terahertz-pulse generation in a laser-generated nitrogen plasma. *J. Appl. Phys.* **91**, 2611-2614 (2002).
- ⁷ Cook, D. J., and Hochstrasser, R. M. Intense terahertz pulses by four-wave rectification in air. *Opt. Lett.* **25**, 1210-1212 (2000).
- ⁸ Kreß, M., Löffler, T., Eden, S., Thomson, M. and Roskos, H. G. Terahertz-pulse generation by photoionization of air with laser pulses composed of both fundamental and second-harmonic wave. *Opt. Lett.* **29**, 1120-1122 (2004).
- ⁹ Bartel, T., Gaal, P., Reimann, K., Woerner, M., and Elsaesser, T. Generation of single-cycle THz transients with high electric-field amplitudes, *Opt. Lett.* **30**, 2805-2807 (2005).
- ¹⁰ Xie, X., Dai, J., and Zhang, X.-C. Coherent Control of THz Wave Generation in Ambient Air, *Phys. Rev. Lett.* **96**, 075005 (2006).
- ¹¹ Itatani, J., Zeidler, D., Levesque, J., Spanner, M., Villeneuve, D. M., and Corkum, P. B. Controlling High Harmonic Generation with Molecular Wave Packets, *Phys. Rev. Lett.* **94**, 123902 (2005).
- ¹² Macklin, J. J., Kmetec, J. D., and Gordon III, C. L. High-Order Harmonic Generation Using Intense Femtosecond Pulses. *Phys. Rev. Lett.* **70**, 766-769 (1993).
- ¹³ Gordienko, S., Pukhov, A., Shorokhov, O., and Beava, T. Relativistic Doppler Effect: Universal Spectra and Zep-tosecond Pulses, *Phys. Rev. Lett.* **93**, 115002 (2004).
- ¹⁴ Itatani, J., Levesque, J., Zeidler, D., Niikura, H., Pepin, H., Kieffer, J. C., Corkum, P. B. and Villeneuve, D. M. Tomographic imaging of molecular orbitals, *Nature* **432**, 867-871 (2004).
- ¹⁵ Pukhov, A., and Meyer-ter-Vehn, J. Laser Wake Field Acceleration: The High Non-Linear Broken-Wave Regime, *Appl. Phys. B* **74**, 355-361 (2002), Mangles, S. P. D., *et al.* Monoenergetic beams of relativistic electrons from intense laser-plasma interactions, *Nature* **431**, 535-538 (2004), Geddes, C. G. R., *et al.* High-quality electron beams from a laser wakefield accelerator using plasma-channel guiding, *Nature* **431**, 538-541 (2004), Faure, J., *et al.* A laser-plasma accelerator producing monoenergetic electron beams, *Nature* **431**, 541 (2004).
- ¹⁶ Liu, X. *et al.* Nonsequential double ionization at the single-optical-cycle limit, *Phys. Rev. Lett.* **93**, 263001 (2004).
- ¹⁷ Lindner, F., Paulus, G. G., Walther, H., Baltuška, A., Goulielmakes, E., Lezius, M., and Krausz, F. Gouy-Phase Shift for Few-Cycle Laser Pulses, *Phys. Rev. Lett.* **92**, 113001 (2004).
- ¹⁸ Roos, P.A., Li, X., Smith, R. P., Pipis, J. A., Fortier, T. M., and Cundiff, S. T. Solid-state carrier-envelope phase stabilization via quantum interference control of injected photocurrents. *Optics Letters* **30**, 735-737, (2005).
- ¹⁹ Bandrauk, A. D., Chelkowski, S., Nguyen, H. S. Attosecond localization in molecules, *Int. J. of Quant. Chem.* **100**, 834-844 (2004).
- ²⁰ Paulus, G. G., Lindner, F., Walther, H., Baltuška, A.,

- Goulielmakis, E., Lezius, M., and Krausz, F. Measurement of the Phase of Few-Cycle Laser Pulses, *Phys. Rev. Lett.* **91**, 253004 (2003).
- ²¹ Paulus, G. G. A Meter of the “Absolute” Phase of Few-Cycle Pulses, *Laser Physics* **15**, 843-854 (2005).
- ²² Hamster, H., Sullivan, A., Gordon, S., White, W., and Falcone, R. W. Subpicosecond electromagnetic pulses from intense laser-plasma interaction, *Phys. Rev. Lett.* **71**, 2725-2728 (1993).
- ²³ Corkum, P. B., Burnett, N. H. and Brunel, F. Above-threshold ionization in the long-wavelength limit, *Phys. Rev. Lett.* **62**, 1259-1262 (1989).
- ²⁴ Löffler, T., Kreß, M., Thomson, M., and Roskos H. G. Efficient Terahertz Pulse Generation in Laser-Induced Gas Plasmas, *Act. Phys. Pol. A*, **107**, 99-108 (2005).
- ²⁵ Guo, C., Li, M., Nibarger, J. P. and Gibson, G. N. Single and double ionization of diatomic molecules in strong laser fields, *Phys. Rev. A* **58**, 4271-4274 (1998).
- ²⁶ Biondi, M. A. and Brown, S. C. Measurement of electron-ion recombination, *Phys. Rev.* **76**, 1697-1700 (1949).
- ²⁷ Shvartsburg, A. B. *Time-domain Optics of Ultrashort Waveforms*, (Oxford Series in Optical Sciences No.10),(Oxford Univ. Press, Oxford, 1996).

Acknowledgements

We would like to acknowledge fruitful discussions with M. Horbatsch from York University, Canada. This work was supported in part by the Hochschulförderungsprogramm of GSI Darmstadt and by the Deutsche Forschungsgemeinschaft within the contract Mo850/2 (U.M.). Support from the Leibniz-Program of the Deutsche Forschungsgemeinschaft (J.U.) is gratefully acknowledged.

Competing interests statement

The authors declare that they have no competing financial interests.